

**Computer-aided discovery, validation and mechanistic characterisation  
of novel neolignan activators of PPAR $\gamma$**

**Nanang Fakhrudin<sup>1,2</sup>, Angela Ladurner<sup>1</sup>, Atanas G. Atanasov, Elke H. Heiss, Lisa  
Baumgartner, Patrick Markt, Daniela Schuster, Ernst P. Ellmerer, Gerhard Wolber,  
Judith M. Rollinger, Hermann Stuppner, Verena M. Dirsch**

*Department of Pharmacognosy, Faculty of Life Sciences, University of Vienna, Austria*

*(N.F., A.L., A.G.A., E.H.H., V.M.D.)*

*Institute of Pharmacy/Pharmacognosy and Center for Molecular Biosciences Innsbruck,*

*University of Innsbruck, Austria (L.B., J.M.R., H.S.)*

*Institute of Pharmacy/Pharmaceutical Chemistry and Center for Molecular Biosciences*

*Innsbruck, University of Innsbruck, Austria (P.M., D.S., G.W.)*

*Institute of Organic Chemistry, University of Innsbruck, Austria (E.P.E.)*

*Inte:Ligand GmbH, Vienna, Austria (P.M., G.W.)*

MOL 62141

**Running title:** PPAR $\gamma$  and neolignans

**Corresponding author:** Atanas Georgiev Atanasov, University of Vienna, Department of Pharmacognosy, Faculty of Life Sciences, Althanstrasse 14, 1090 Vienna, Austria.

Tel.: +43-1-4277-55226

Fax: +43-1-4277-9552

E-mail: atanas.atanasov@univie.ac.at

**Document statistics:**

Number of text pages: 30

Number of tables: 1

Number of figures: 6

Number of references: 38

Number of words in the Abstract: 219

Number of words in the Introduction: 531

Number of words in the Discussion: 943

**List of abbreviations:** BADGE, bisphenol A diglycidyl ether; CC, column chromatography; CHM, 3D natural product database of Chinese herbal medicine; DIOS, 3D natural product database based on Dioscorides *De materia medica*; DMEM, Dulbecco's modified Eagle's medium; DMSO, dimethyl sulfoxide; EGFP, enhanced green fluorescent protein; GST, glutathione-S-transferase; *K<sub>i</sub>*, inhibition constant; LBD, ligand binding domain; NMR, nuclear magnetic resonance; PDB, Protein Data Bank; PPAR, peroxisome proliferator-activated receptor; PPRE, PPAR response elements; RXR, retinoid X receptor; TR-FRET, time-resolved fluorescence resonance energy transfer; TZD, thiazolidinedione.

MOL 62141

## Abstract

Peroxisome proliferator-activated receptor gamma (PPAR $\gamma$ ) agonists are used for the treatment of type 2 diabetes and metabolic syndrome. However, the currently used PPAR $\gamma$  agonists display serious side effects leading to a great interest in the discovery of novel ligands with favourable properties. Aim of our study was to identify new PPAR $\gamma$  agonists by a PPAR $\gamma$  pharmacophore-based virtual screening of 3D natural product libraries. This *in silico* approach led to the identification of several neolignans predicted to bind the receptor ligand binding domain (LBD). To confirm this prediction, the neolignans dieugenol, tetrahydrodieugenol, and magnolol were isolated from the respective natural source or synthesized and subsequently tested for PPAR $\gamma$  receptor binding. The neolignans bound to the PPAR $\gamma$  LBD with EC<sub>50</sub>s in the nanomolar range, exhibiting a binding pattern highly similar to the clinically used agonist pioglitazone. In intact cells, dieugenol and tetrahydrodieugenol selectively activated hPPAR $\gamma$ -, but not hPPAR $\alpha$ - or hPPAR $\beta/\delta$ -mediated luciferase reporter expression, with a pattern suggesting partial PPAR $\gamma$  agonism. The coactivator recruitment study also demonstrated partial agonism of the tested neolignans. Dieugenol, tetrahydrodieugenol, and magnolol but not the structurally related eugenol induced 3T3-L1 preadipocyte differentiation confirming effectiveness in a cell model with endogenous PPAR $\gamma$  expression. In conclusion, we identified neolignans as novel ligands for PPAR $\gamma$ , which exhibited interesting activation profiles, recommending them as potential pharmaceutical leads or dietary supplements.

MOL 62141

## Introduction

Western lifestyle with a high intake of simple sugars, saturated fat, and physical inactivity promotes pathologic conditions such as type 2 diabetes, obesity and metabolic syndrome, which are currently taking a devastating epidemical spread worldwide. Compounds that are activating PPAR $\gamma$  may help to fight these pathological conditions (Cho and Momose, 2008).

PPARs are ligand-activated transcription factors belonging to the nuclear receptor superfamily, and their main function relates to the regulation of genes involved in glucose and lipid metabolism (Desvergne et al., 2006; Tenenbaum et al., 2003). Three isoforms of this nuclear receptor have been identified so far: PPAR $\alpha$ , PPAR $\beta/\delta$ , and PPAR $\gamma$ . PPAR $\alpha$  is highly expressed in skeletal muscle, liver, kidney, heart, and the vascular wall and it was shown to be mainly involved in the regulation of lipid catabolism (Fruchart, 2009). PPAR $\gamma$  is predominantly expressed in adipose tissue and its activation promotes adipogenesis and increases insulin sensitivity (Anghel and Wahli, 2007). More recently, PPAR $\gamma$  has been shown to be involved in the regulation of genes contributing to inflammation, hypertension, and atherosclerosis (Gurnell, 2007). PPAR $\beta/\delta$  has a broader expression pattern and is involved in the regulation of lipid metabolism and energy expenditure (Bedu et al., 2005; Luquet et al., 2005).

Once activated by their ligands, the PPARs translocate into the nucleus, form heterodimers with the retinoid X receptor (RXR), and subsequently bind to PPAR response elements (PPREs) that are located in the promoter regions of PPAR-responsive target genes (Bardot et al., 1993). Binding of the PPAR-RXR heterodimers to the PPREs triggers further recruitment of diverse nuclear receptor coactivators (SRC-1, TRAP220, CBP, p300, PGS-1, and/or others), contributing to the transcriptional regulation of the target genes (Yu and Reddy, 2007).

MOL 62141

PPAR $\gamma$  activators are currently used as insulin sensitizers to combat type 2 diabetes and metabolic syndrome (Cho and Momose, 2008). However, the PPAR $\gamma$  agonists in clinical use, represented by thiazolidinediones (TZDs), have serious side effects such as weight gain, increased bone fracture, fluid retention, and heart failure (Rizos et al., 2009). Therefore, the discovery and optimization of new PPAR $\gamma$  agonists that would display reduced side effects is of great interest. TZDs are full PPAR $\gamma$  agonists inducing maximal receptor activation. Of note, partial PPAR $\gamma$  agonists recently came into focus as a possible new generation of promising PPAR $\gamma$  ligands. Partial agonists induce alternative receptor conformations and thus recruit different coactivators resulting in distinct transcriptional effects compared to TZDs. There are firm indications that such partial agonists might retain the needed effectiveness while having reduced side effects (Chang et al., 2007; Yumuk, 2006).

Natural products are an important and promising source for drug discovery (Newman and Cragg, 2007). Aim of our study was, therefore, to identify natural products that activate human PPAR $\gamma$  (hPPAR $\gamma$ ) acting possibly as partial agonists. To achieve this objective, we used an *in silico* approach making use of a pharmacophore model for hPPAR $\gamma$  developed previously (Markt et al., 2008; Markt et al., 2007) and 3D databases of natural products. The conducted virtual screen utilizing two 3D databases and the pharmacophore model led to the identification of neolignans. The three neolignans dieugenol, tetrahydrodieugenol, and magnolol were isolated from the respective natural source or synthesized and characterized in several PPAR $\gamma$ -specific *in vitro* models or intact cells.

MOL 62141

## **Materials and Methods**

### **Chemicals, cell culture reagents, and plasmids**

Dulbecco's modified Eagle's medium (DMEM) containing 4.5 g/l glucose was purchased from Lonza (Basel, Switzerland). The fetal bovine serum was from Gibco (Invitrogen, Lofer, Austria). GW7647, GW0742 and BADGE were purchased from Cayman Europe. Pioglitazone was purchased from Molekula Ltd (Shaftesbury, UK). All other chemicals were obtained from Sigma–Aldrich (Vienna, Austria). The test compounds were dissolved in DMSO, aliquoted and kept frozen until use. In all test models a solvent vehicle control was always included to assure that DMSO does not interfere with the respective model. For all cell-based assays the final concentration of DMSO was kept 0.1% or lower. The PPAR luciferase reporter construct (tk-PPREx3-luc) and the expression plasmid for murine PPAR $\gamma$  (pCMX-mPPAR $\gamma$ ) were a kind gift from Prof. Ronald M. Evans (Howard Hughes Medical Institute, California), the plasmid encoding enhanced green fluorescent protein (pEGFP-N1) was obtained from Clontech, and the expression plasmids for the three human PPAR subtypes (pSG5-PL-hPPAR-alpha, pSG5-hPPAR-beta, pSG5-PL-hPPAR-gamma1) were a kind gift from Prof. Walter Wahli and Prof. Beatrice Desvergne (Center for Integrative Genomics, University of Lausanne, Switzerland).

### **Pharmacophore-based Virtual Screening**

The pharmacophore model used for virtual screening was taken from the model collection reported previously (Markt et al., 2008; Markt et al., 2007). Data mining of the natural product databases was performed using Catalyst 4.11. For virtual screening, the fast flexible search algorithm of Catalyst was used.

### **Virtual natural product databases**

MOL 62141

The two virtual 3D compound databases used in this study have been generated previously. The DIOS database contains 9676 individual small-molecular weight natural products found in ancient herbal medicines described in *De materia medica*, by Pedanius Dioscorides (1<sup>st</sup> cent. AD) (Rollinger et al., 2008). The Chinese Herbal Medicine (CHM) database contains 10216 compounds which are reported to be contained in medicinal preparations used in traditional Chinese medicine. Both 3D databases were generated within Catalyst. 3D structures of the compounds were built and consequently energetically minimized using the structure editor of Catalyst. The catConf algorithm was applied to create conformational models for the compounds using the following settings: maximum number of conformers = 100, generation type = fast quality, and energy range = 20 kcal/mol above the calculated lowest energy conformation.

### Isolation

Magnolol (**3**) was isolated from the bark of *Magnolia officinalis* Rehd. & Wils. The plant material provided by Plantasia (Oberndorf, Austria) corresponded to the quality described at the Chinese Pharmacopoeia. 880 g powdered bark of *Magnolia officinalis* (Plantasia, Oberndorf, Austria; Ch.Nr. 710786) were exhaustively macerated with dichloromethane (8.0 l, 12 times, at room temperature) yielding 96.7 g crude extract. 80.0 g of the obtained extract were separated by flash silica gel column chromatography (CC) (400 g silica gel 60, 40-63  $\mu$ m, Merck, VWR, Darmstadt, Germany; 41 x 3.5 cm) using a petroleum ether-acetone gradient with an increasing amount of acetone resulting in 18 fractions (A1-A18). Fraction A5 (17.29 g) was further separated by means of vacuum liquid chromatography (10 x 5 cm) with LiChroprep® RP-18 material (100.0 g; 40-63  $\mu$ m; Merck, Darmstadt, Germany) using an acetonitrile-water gradient with an increasing amount of acetonitrile. Fractions eluted with 45% to 60% acetonitrile were combined (4.19 g) and further separated by Sephadex® LH-20 (Pharmacia Biotech, Sweden) CC using a

MOL 62141

dichloromethane-acetone mixture (85+15, v/v) as mobile phase (subfractions B1-B17). Fraction B13 (3.67 g) was recrystallized from dichloromethane resulting in 2.32 g of **3** as colourless crystals. The compound was identified by mass spectrometry and NMR-spectroscopy (H-NMR purity > 98%). NMR and MS data are provided as online supplementary information.

### **Synthesis of compounds**

Synthesis of dieugenol (**1**) was performed by oxidative dimerization of eugenol (**4**) (Sigma-Aldrich, Germany) as described by Ogata et al. (Ogata et al., 2000) and Marque et al. (Marque et al., 1998). After recrystallization from 2-propanol, isolated **1** was analysed by NMR (H-NMR purity > 99%). Tetrahydrodieugenol (**2**) was synthesized by hydrogenation of **1** in a Parr apparatus at 40 psi as described by Ogata et al. (Ogata et al., 2000). After recrystallization from 2-propanol, compound **2** was analysed by NMR (H-NMR purity > 97%). NMR and MS data of **1** and **2** validating the identification of the two compounds are provided as online supplementary information.

### **PPAR $\gamma$ competitive ligand binding**

The LanthaScreen™ Time-Resolved Fluorescence Resonance Energy Transfer (TR-FRET) PPAR $\gamma$  competitive binding assay (Invitrogen, Lofer, Austria) was performed using the manufacturer's protocol. The test compounds dissolved in DMSO or solvent vehicle were incubated together with the hPPAR $\gamma$  LBD tagged with GST, terbium-labelled anti-GST antibody and fluorescently labelled PPAR $\gamma$  ligand (Fluormone™ Pan-PPAR Green, Invitrogen). In this assay, the fluorescently labelled ligand is binding to the hPPAR $\gamma$  LBD which brings it in a close spatial proximity to the terbium-labelled anti-GST antibody. Excitation of the terbium at 340 nm results in energy transfer (FRET) and partial excitation



MOL 62141

of the fluorescently labelled ligand, followed by emission at 520 nm. Test-compounds binding to the hPPAR $\gamma$  LBD are competing with the fluorescently labelled ligand and displacing it, resulting in a decrease of the FRET signal. The 520 nm signals were normalized to the signals obtained from the terbium emission at 495 nm and therefore the decrease in the 520 nm/495 nm ratios was used as a measure for the ability of the tested compounds to bind to the hPPAR $\gamma$  LBD. All measurements were performed with a GeniosPro plate reader (Tecan, Austria).

### **PPAR luciferase reporter gene transactivation**

HEK-293 cells (ATCC, USA) were grown in DMEM with phenol red supplemented with 584 mg/ml glutamine, 100 U/ml benzylpenicillin, 100  $\mu$ g/ml streptomycin, and 10% fetal bovine serum. Cells were maintained in 75 cm<sup>2</sup> flasks with 10 ml medium at 37°C and 5% CO<sub>2</sub>. For transient transfection, cells were seeded in 10 cm dishes at a density of  $6 \times 10^6$  cells/dish for 18 h, and then transfected by the calcium phosphate precipitation method with 4  $\mu$ g of the respective PPAR receptor expression plasmid, 4  $\mu$ g reporter plasmid (tk-PPREx3-luc), and 2  $\mu$ g green fluorescent protein plasmid (pEGFP-N1) as internal control. The total DNA and the ratio tk-PPREx3-luc:PPAR:EGFP were kept 10  $\mu$ g and 2:2:1, respectively. Six hours after the transfection, cells were harvested and re-seeded in 96-well plates ( $5 \times 10^4$  cells/well) in DMEM without phenol red, supplemented with 584 mg/ml glutamine, 100 U/ml benzylpenicillin, 100  $\mu$ g/ml streptomycin, and 5% charcoal stripped fetal bovine serum. Then cells were treated with the respective compounds and incubated for 18 h. After cell lysis, the luminescence of the firefly luciferase and the fluorescence of EGFP were quantified on a GeniosPro plate reader (Tecan, Austria). The luminescence signals were normalized to the EGFP-derived fluorescence, to account for differences in cell number and/or transfection efficiency.

MOL 62141

### **PPAR $\gamma$ coactivator recruitment**

The LanthaScreen™ TR-FRET PPAR $\gamma$  coactivator assay (Invitrogen, Lofer, Austria) was performed according to the manufacturers' protocol. The test compounds dissolved in DMSO or solvent vehicle were incubated together with fluorescein-labelled TRAP220/DRIP-2 coactivator peptide (Rachez et al., 2000), hPPAR $\gamma$  LBD tagged with GST, and terbium-labelled anti-GST antibody. In this assay the binding of an agonist to hPPAR $\gamma$  LBD results in a conformational change leading to recruitment of the coactivator TRAP220/DRIP-2 peptide. This recruitment brings the fluorescein attached to the coactivator peptide and the terbium attached to the GST antibody in close spatial proximity, and excitation of the terbium at 340 nm results in a FRET and a consequent partial excitation of the fluorescein that is monitored at 520 nm. The 520 nm signals were normalized to the signals obtained from the terbium emission at 495 nm and thus the 520 nm/495 nm ratios were used as a measure for the TRAP220/DRIP-2 coactivator recruitment potential of the tested compounds. All quantifications were performed with a GeniosPro plate reader (Tecan, Austria).

### **Adipocyte differentiation**

3T3-L1 preadipocytes (ATCC, USA) were propagated in DMEM supplemented with 10% calf serum. For differentiation, the preadipocytes were grown to confluence (day -2) and kept for two more days before medium was changed to DMEM supplemented with 10 % fetal calf serum, 1  $\mu$ g/ml insulin, and potential PPAR $\gamma$  activators (day 0). In case we wanted to cross-check PPAR dependency of our observations, the PPAR $\gamma$  antagonist BADGE was added one hour prior to the addition of the potential agonists. Medium was renewed every two days until day 7 or 8. For an estimate of accumulated lipids and thus for the adipogenic potential of the test compounds, Oil Red O staining was performed. For

MOL 62141

this, cells were fixed in 10% formaldehyde for 1 h and stained with Oil Red O for 10 minutes. After washing off the excessive dye, photos were taken, and bound dye was solubilized with 100% isopropanol and photometrically quantified at 550 nm.

### **Molecular Docking**

The molecular docking was performed using the GOLD Suite software package (CCDC, 2008). Extraction and preparation of the human PPAR $\gamma$  ligand binding pocket for the docking of two molecules of dieugenol (**1**), tetrahydrodieugenol (**2**), and magnolol (**3**) simultaneously, was done within this software package. To find a suitable ligand binding pocket, we examined the Brookhaven Protein Data Bank (PDB) (Berman et al., 2000) for crystal structures of a PPAR $\gamma$ -ligand complexes. The PDB entry 2vsr provides the X-ray data with the best resolution among all PPAR $\gamma$ -ligand complexes including two copies of the ligand binding simultaneously to their ligand binding pocket. Thus, we used the ligand binding pocket of this PDB complex for molecular docking. For ligand preparation, we applied Corina 3.00 (Molecular\_Networks, 2009) and the ilib framework (Wolber and Langer, 2001) to generate 3D structures, and to calculate the protonation states of the neolignans at physiological pH, respectively. The best docking poses were selected based on their GOLDScores and their plausibility. Thus, if a docking pose represented PPAR $\gamma$ -ligand interactions well known from literature, the pose was determined to be more realistic than a higher scored docking pose including unknown and implausible protein-ligand interactions. Finally, the docking pose and the interactions with the binding site were visualized using the LigandScout software 2.0. (Wolber et al., 2006; Wolber and Langer, 2005).

### **Statistical methods and data analysis**

MOL 62141

Statistical analysis and non linear regression (with settings for sigmoidal dose response and variable slope) were done using GraphPad Prism software version 4.03 (GraphPad Software Inc, USA). One-way Analysis of Variance (ANOVA) with Bonferroni post test was used to calculate the statistical significance. For comparison of just two experimental conditions, two-tailed paired t-test was applied. Results with  $p < 0.05$  were considered significant.  $K_i$  values of competitor compounds were also calculated with the GraphPad Prism software version 4.03 utilizing Cheng-Prusoff equation ( $K_i = IC_{50}/(1 + L/KD)$ ).

## Results

### Pharmacophore-based virtual screening

To identify new natural product-derived PPAR $\gamma$  ligands we used a pharmacophore-based virtual screening approach. The generation and experimental validation of the pharmacophore models were described previously (Markt et al., 2008; Markt et al., 2007). For our study, the best pharmacophore model for PPAR $\gamma$  partial agonists based on the PDB entry 2g0g (Lu et al., 2006) was selected. The generated model consists of three hydrophobic features, one aromatic ring, one hydrogen bond acceptor, and exclusion volume spheres lining the ligand binding domain of PPAR $\gamma$ . Virtual screening of the 3D multi-conformational natural product databases DIOS and CHM resulted in 34 (0.4%) and 27 (0.3%) hits, respectively. Highly scored virtual hits were obtained from the chemical class of neolignans. The small molecular weight compounds dieugenol (**1**) and tetrahydrodieugenol (**2**), both representing dimers of the abundant natural phenylpropanoid eugenol (**4**), were selected from the hit list. A further neolignan with highly similar structure, magnolol (**3**), which is a prominent constituent of the traditional Chinese herbal remedy magnolia bark (hòu pò), has also been selected for pharmacological evaluation (Fig. 1).

MOL 62141

### Isolation and synthesis of compounds

The synthesis of **1** was performed by oxidative dimerization of **4** as previously described. After recrystallization from 2-propanol the isolated **1** was analyzed by NMR. The melting point was found at 101-104 °C (cf. Crossfire BRN 2061706 m.p. between 93 and 108 °C), and the NMR data are in accordance with the published data (Marque et al., 1998; Ogata et al., 2000). Synthesis of **2** was performed by hydrogenation of **1** as described by Ogata et al. (Ogata et al., 2000). After recrystallization from 2-propanol the melting point (147-149 °C) and the NMR data are in accordance with the published data (Ogata et al., 2000).

The isolation of **3** from the bark of *Magnolia officinalis* Rehd. & Wils using different chromatographic methods yielded 0.26%. The compound was identified by mass spectrometry and NMR-spectroscopy and had physical and spectroscopic properties consistent with the literature (Yahara et al., 1991).

### PPAR $\gamma$ ligand binding

To validate the predicted hits from the virtual screening approach, we first studied the ability of the neolignans to bind to the purified hPPAR $\gamma$  LBD, assessed by a LanthaScreen™ TR-FRET PPAR $\gamma$  competitive binding assay. Dose-response studies were performed with **1-4** (Fig. 2). Stronger binding of the tested compound to the PPAR $\gamma$  LBD in this assay results in a stronger displacement of the fluorescently labelled ligand (Fluormone™ Pan-PPAR Green, Invitrogen) leading to a decrease of the FRET signal. Pioglitazone (Actos®), a selective PPAR $\gamma$  agonist in clinical use, was used as positive control. **1-3** showed binding properties similar to pioglitazone, while **4** did not bind to the receptor at all (at test concentrations up to 100  $\mu$ M). Interestingly, compounds **1** and **2** were binding to the hPPAR $\gamma$  LBD with even higher affinity ( $K_i$  values of 0.24  $\mu$ M and

MOL 62141

0.32  $\mu\text{M}$ , respectively) than pioglitazone ( $K_i = 1.19 \mu\text{M}$ ), whereas **3** was binding with a slightly lower affinity ( $K_i = 2.04 \mu\text{M}$ ).

### **PPAR $\gamma$ luciferase reporter gene transactivation**

To assess whether the neolignans are able to act as functional PPAR $\gamma$  agonists in intact cells, we next performed PPAR $\gamma$  luciferase reporter gene assays. HEK-293 cells were cotransfected with a hPPAR $\gamma$  expression plasmid, a PPAR luciferase reporter plasmid (tk-PPREx3-luc), and EGFP as an internal control. Compounds **1-3** induced a dose-dependent activation of PPAR $\gamma$  in a concentration range similar to pioglitazone (Fig. 3). The maximal activation in response to **1-2** and pioglitazone was achieved with similar concentrations (about 1  $\mu\text{M}$  from the respective compound to reach saturation response), indicating again similar binding affinities to PPAR $\gamma$ . The maximal fold activation by **1-2**, however, was several folds lower than by the full agonist pioglitazone, indicating a partial agonism of the neolignans in this test system.

### **PPAR $\gamma$ coactivator recruitment**

The binding of ligands to the PPAR $\gamma$  LBD results in a conformational change of the receptor and subsequent recruitment of coactivator proteins (TRAP220, SRC-1, CBP, p300, PGS-1, and/or others), that contribute to the transcriptional regulation of the different PPAR-responsive promoters (Yu and Reddy, 2007). To assess whether the lower maximal activation achieved by the neolignans in the luciferase reporter gene assay might be due to differences in the coactivator recruitment potential of the formed ligand-receptor complex, we next performed a TRAP220/DRIP-2 coactivator recruitment assay.

As shown in Figure 4, indeed compounds **1-3** induced just a partial recruitment of the fluorescein-labelled TRAP220/DRIP-2 coactivator peptide to the PPAR $\gamma$  LBD, whereas

MOL 62141

the known full PPAR $\gamma$  agonist pioglitazone induced a several fold stronger activation. As expected, compound **4** again was not active. In agreement with the result from the luciferase reporter gene assay, the concentration range needed for a saturation response was highly similar for compounds **1-3** and pioglitazone. However, the maximal activation induced with the full agonist pioglitazone was again several times higher.

Taken together, the data obtained from the receptor binding, the luciferase reporter gene transactivation, and the coactivator recruitment are indicating that the neolignans **1-3** are binding to the PPAR $\gamma$  LBD with a high affinity, in a concentration range similar to that of the clinically used agonist pioglitazone (Actos<sup>®</sup>). The conformation of the ligand-receptor complex formed with **1-3** is, however, different than the one induced with the full agonist pioglitazone and as a consequence the neolignans exhibit partial agonism with respect to TRAP220/DRIP-2 coactivator recruitment and tk-PPREx3 promoter activation.

### **Molecular docking**

To get a deeper mechanistic understanding of the binding of **1-3** to the PPAR $\gamma$  ligand binding pocket, we examined the putative binding modes of these ligands *in silico* by docking them into the hPPAR $\gamma$  binding pocket. The initial docking of **1-3** to the PPAR $\gamma$  binding pocket showed that these small PPAR $\gamma$  ligands occupy only a minor part of the large ligand binding pocket, and thus leave space and hydrogen bond possibilities for a second ligand. Recently, Itoh et al. (Itoh et al., 2008) crystallized a PPAR $\gamma$ -ligand complex containing a fatty acid bound to the ligand binding pocket in a dimeric way. Based on this new information, we have assumed for our docking studies that the agonistic activity of **1-3** is caused by the simultaneous binding of two copies of this ligand to the binding site. From docking compound **1** into the PPAR $\gamma$  ligand binding pocket twice, several hydrogen bonds between the two dieugenol ligands and the binding site can be observed (Fig. 5A).

MOL 62141

Ser289 and Cys285 form a hydrogen bond network with one 2-methoxyphenol moiety of the molecule of **1** that is located next to arm I, as visualized in Fig 5A. The second part of the ligand dimer establishes several hydrogen bonds between residues Ser342 and Glu343 and one of its 2-methoxyphenol moieties. The other 2-methoxyphenol group of this copy of **1** is involved in a hydrogen bond network formed between both ligands. In addition, the vinyl, phenyl, and methoxy moieties of both molecules established hydrophobic contacts to the binding pocket.

Next, two molecules of **2** were docked to the ligand binding pocket, which resulted in the prediction of a binding mode including similar protein-ligand interactions as described for **1** (Fig. 5B).

The best docking pose for compound **3** consisted of one copy of **3** located between arm I and arm III and the other part of the ligand dimer situated between arm II and arm III (Fig. 5C). The molecule of **3** oriented towards arm I forms hydrogen bonds between one hydroxyl group and residues Ser289 and Cys285. Both hydroxyl groups of this copy of **3** are involved in hydrogen bonding with one hydroxyl group of the second part of the dimer. The remaining hydroxyl group of the latter ligand formed another hydrogen bond to residue Gly284. In addition, both molecules establish several hydrophobic interactions with the three arms of the binding pocket.

Similar docking poses determined for **1** and **2** show that the putative binding modes for both compounds include more interactions with the PPAR $\gamma$  binding pocket than the predicted binding mode for compound **3**. This could be an explanation for the higher affinity of **1** and **2** compared to **3**.

### Selectivity of action

We next studied whether the neolignans are activating PPAR $\gamma$  selectively over the other two PPAR subtypes. The subtype specificity of the assay was achieved by replacing the



MOL 62141

expression plasmid for hPPAR $\gamma$  with an expression plasmid for hPPAR $\alpha$  and hPPAR $\beta/\delta$ , respectively (Table 1). Mouse PPAR $\gamma$  (mPPAR $\gamma$ ) was also tested to exclude species differences that could modulate the effectiveness of neolignans in PPAR $\gamma$  experimental models from rodent origin, such as the 3T3-L1 cells that we used (Fig. 6). The specificity of the assays was verified with known selective agonists of PPAR $\alpha$  (GW7647), PPAR $\beta/\delta$  (GW0742), and PPAR $\gamma$  (pioglitazone). **1-3** activated PPAR $\gamma$  3.58-fold (with an EC<sub>50</sub> of 0.62  $\mu$ M), 3.34-fold (with an EC<sub>50</sub> of 0.33  $\mu$ M) and 3.03-fold (with an EC<sub>50</sub> of 1.62  $\mu$ M), respectively. Highly similar activation was seen with mPPAR $\gamma$ , suggesting that the neolignans have very comparable potency of action also with the rodent receptor. Compound **4** had no effect on any of the PPAR subtypes tested. The positive control for PPAR $\gamma$ , pioglitazone, induced an 8.05-fold activation (EC<sub>50</sub> of 0.26  $\mu$ M) with hPPAR $\gamma$  and a 6.80-fold activation (EC<sub>50</sub> of 0.22  $\mu$ M) with mPPAR $\gamma$ . Interestingly, **1** and **2** activated PPAR $\gamma$  selectively with no effect on the other two PPAR subtypes. Compound **3** was not equally specific, since it was activating also hPPAR $\beta/\delta$  at higher concentrations.

### Adipocyte differentiation

We next aimed to confirm the effectiveness of the neolignans in a functionally relevant cell model with endogenous expression of PPAR $\gamma$ . Since it is known that PPAR $\gamma$  is an essential player in adipocyte differentiation (Rosen et al., 1999) we examined the adipogenic potential of **1-4** in 3T3-L1 preadipocytes. As positive control we chose rosiglitazone (1  $\mu$ M) the most often used control TZD in this model (Fig. 6A, 6B) (Wright et al., 2000). As evident by the accumulation of lipid droplets and subsequent Oil Red staining, the treatment with 10  $\mu$ M of **1-3** resulted in the differentiation to adipocytes, whereas **4** had no adipogenic activity (Fig. 6A). Furthermore, the PPAR $\gamma$  antagonist BADGE (Wright et al.,

MOL 62141

2000) significantly reduced the adipogenic potential of **1-3** and the positive control rosiglitazone, demonstrating PPAR $\gamma$  dependency of the observed effect (Fig. 6B).

## Discussion

Here we show the identification of several neolignans that act as partial PPAR $\gamma$  agonists using an *in silico* approach including a pharmacophore-based virtual screening of the natural product databases DIOS and CHM (Rollinger et al., 2008).

The affinity of the virtual hits for the hPPAR $\gamma$  LBD was experimentally confirmed in a PPAR $\gamma$  competitive ligand binding assay (Fig. 2). Compounds **1-3** potently bind to the receptor LBD in a concentration range similar to that of the clinically used PPAR $\gamma$  agonist pioglitazone (Actos<sup>®</sup>). Based on these promising *in vitro* results we further verified the ability of these neolignans to activate PPAR $\gamma$  also in a cellular model. Indeed, **1-3** dose-dependently activated hPPAR $\gamma$  in a HEK-293 cell-based luciferase reporter gene transactivation model (Fig. 3). The concentrations needed to reach a saturation response by compounds **1-3** were similar to that of pioglitazone indicating again a similar affinity to the PPAR $\gamma$  receptor binding pocket. The maximal activation reached by pioglitazone, however, was several fold higher indicating that the neolignans are acting as partial PPAR $\gamma$  agonists in this model. It is well known, that different PPAR ligands might form ligand-receptor complexes with different coactivator recruitment potentials and thus different transactivation properties. We, therefore, studied the TRAP220/DRIP-2 coactivator recruitment properties of the PPAR $\gamma$ -ligand complexes induced by the neolignans in comparison to the known full agonist pioglitazone (Fig. 4). The neolignans **1-3** again acted as partial agonists, since the maximal activation was several fold lower than the activation induced by the full TZD agonist. Thus, compared to pioglitazone, the neolignans **1-3** possess a similar affinity to PPAR $\gamma$  but apparently induce a receptor-ligand complex with a

MOL 62141

different conformation leading to partial agonism. TZDs that are currently clinically used as PPAR $\gamma$  activators are potent full agonists of PPAR $\gamma$ . To avoid the undesired side effects of TZDs, the development of novel partial PPAR $\gamma$  agonists was suggested as a highly promising approach (Chang et al., 2007; Yumuk, 2006). Thus, MBX-102 (metaglidase), a selective partial PPAR $\gamma$  agonist, exhibiting a weaker transactivation activity and a reduced coactivator recruitment potential, was recently reported to retain antidiabetic properties in the absence of weight gain and edema (Gregoire et al., 2009). The activation pattern of the neolignans makes them, therefore, a highly interesting class of PPAR $\gamma$  activators.

In all systems used, **1** and **2** had the highest potency among the tested neolignans, closely followed by **3**, whereas **4** had no activity. To get a deeper insight into the binding mode of the neolignans to the hPPAR $\gamma$  LBD, we utilized molecular docking (Fig. 5). The docking studies assume the neolignans to bind as dimers to the receptor binding pocket, and reveal **1** and **2** to make more interactions with the PPAR $\gamma$  binding pocket than **3**, underlining the higher activity observed with these compounds.

**1** and **2** selectively activated hPPAR $\gamma$  but not hPPAR $\beta/\delta$  or hPPAR $\alpha$  (Table 1). This is another favourable profile of action since all PPAR $\gamma$  agonists that are currently approved on the market are isoform specific PPAR $\gamma$  activators. There are though some experimental indications that PPAR dual-agonists or pan-agonists might also provide advantages (Chang et al., 2007).

Since the PPAR luciferase reporter gene assay represents an artificial cell model with transient overexpression of PPAR $\gamma$ , we examined all neolignans for their ability to differentiate 3T3-L1 adipocytes, which is a functionally relevant cell model making use of endogenously expressed PPAR $\gamma$ . In line with the results from all other models, **1-3** induced adipocyte differentiation and their activity was abolished by the PPAR antagonist BADGE.

MOL 62141

Compound **4** was, however, not active, again confirming the results from all previous experimental models as well as the predictions from the molecular docking studies.

In addition to our findings shown here, the compounds dieugenol (**1**) and tetrahydrodieugenol (**2**), have been reported previously to act as antioxidants (Ogata et al., 2000), antimutagenics (Miyazawa and Hisama, 2003), and to exert anti-inflammatory activity (Murakami et al., 2003). Magnolol (**3**) is a prominent constituent of the traditional Chinese herbal remedy *magnolia bark* (hòu pò) (Bensky et al., 2004). From a western perspective *Magnolia bark* was suggested to be among the herbal drugs effective in combating metabolic syndrome (Banos et al., 2008). In a recent study, treatment with magnolol decreased fasting blood glucose and plasma insulin levels, and was able to prevent or retard the pathological complications in type 2 diabetic Goto-Kakizaki rats (Sohn et al., 2007). A recent report also showed that magnolol enhances adipocyte differentiation in 3T3-L1 cells and C3H10T1/2 cells, and suggested that these effects might be due to PPAR $\gamma$  modulation (Choi et al., 2009). Here we show that magnolol indeed activates PPAR $\gamma$  in several *in vitro* or cell-based models, but distinct from **1** and **2**, it acts as a dual agonist activating also PPAR $\beta/\delta$  at higher concentrations (Table 1). Although magnolol was not the most potent and specifically acting neolignan in our study, its PPAR activating potential is of interest, since it fits well to the traditional use of *magnolia bark* as a herbal drug combating metabolic disorders.

In summary, we describe the computer-aided discovery of several neolignans as novel ligands of PPAR $\gamma$ . In receptor binding assays, dieugenol (**1**) and tetrahydrodieugenol (**2**) exhibited a higher affinity for PPAR $\gamma$  than the clinically used agonist pioglitazone (Actos<sup>®</sup>). Furthermore, **1** and **2** were identified as selective activators of PPAR $\gamma$ , but not of PPAR $\alpha$  or PPAR $\beta/\delta$ . In comparison to the TZD pioglitazone, **1** and **2** displayed a partial agonism with respect to PPAR $\gamma$  luciferase reporter gene transactivation and

MOL 62141

TRAP220/DRIP-2 coactivator recruitment. In addition, they induced adipocyte differentiation in 3T3-L1 cells PPAR $\gamma$ -dependently. The activation pattern exhibited from **1** and **2** makes them highly interesting novel PPAR $\gamma$  agonists, having the potential to be further explored as leads for the development of novel pharmaceuticals or dietary supplements.

### **Acknowledgments**

We thank Prof. Walter Wahli and Prof. Beatrice Desvergne (Center for Integrative Genomics, University of Lausanne, Switzerland), as well as Prof. Ronald M. Evans (Howard Hughes Medical Institute, California) for providing us with the respective PPAR expression plasmids and the PPRE luciferase reporter construct.

We thank Elisabeth Geiger, Daniel Schachner, and Judith Benedics for excellent technical support.

MOL 62141

## References

- Anghel SI and Wahli W (2007) Fat poetry: a kingdom for PPAR gamma. *Cell Res* **17**:486-511.
- Banos G, Perez-Torres I and El Hafidi M (2008) Medicinal agents in the metabolic syndrome. *Cardiovasc Hematol Agents Med Chem* **6**:237-252.
- Bardot O, Aldridge TC, Latruffe N and Green S (1993) PPAR-RXR heterodimer activates a peroxisome proliferator response element upstream of the bifunctional enzyme gene. *Biochem Biophys Res Commun* **192**:37-45.
- Bedu E, Wahli W and Desvergne B (2005) Peroxisome proliferator-activated receptor beta/delta as a therapeutic target for metabolic diseases. *Expert Opin Ther Targets* **9**:861-873.
- Bensky D, Clavey S and Stöger E (2004) *Chinese Herbal Medicine - Materia Medica*. Eastland Press, Inc., Seattle, WA.
- Berman HM, Westbrook J, Feng Z, Gilliland G, Bhat TN, Weissig H, Shindyalov IN and Bourne PE (2000) The Protein Data Bank. *Nucleic Acids Res* **28**:235-242.
- CCDC (2008) Gold Suite, Cambridge, UK.
- Chang F, Jaber LA, Berlie HD and O'Connell MB (2007) Evolution of peroxisome proliferator-activated receptor agonists. *Ann Pharmacother* **41**:973-983.
- Cho N and Momose Y (2008) Peroxisome proliferator-activated receptor gamma agonists as insulin sensitizers: from the discovery to recent progress. *Curr Top Med Chem* **8**:1483-1507.
- Choi SS, Cha BY, Lee YS, Yonezawa T, Teruya T, Nagai K and Woo JT (2009) Magnolol enhances adipocyte differentiation and glucose uptake in 3T3-L1 cells. *Life Sci*.
- Desvergne B, Michalik L and Wahli W (2006) Transcriptional regulation of metabolism. *Physiol Rev* **86**:465-514.

MOL 62141

- Fruchart JC (2009) Peroxisome proliferator-activated receptor-alpha (PPARalpha): at the crossroads of obesity, diabetes and cardiovascular disease. *Atherosclerosis* **205**:1-8.
- Gregoire FM, Zhang F, Clarke HJ, Gustafson TA, Sears DD, Favelyukis S, Lenhard J, Rentzeperis D, Clemens LE, Mu Y and Lavan BE (2009) MBX-102/JNJ39659100, a novel peroxisome proliferator-activated receptor-ligand with weak transactivation activity retains antidiabetic properties in the absence of weight gain and edema. *Mol Endocrinol* **23**:975-988.
- Gurnell M (2007) 'Striking the Right Balance' in Targeting PPARgamma in the Metabolic Syndrome: Novel Insights from Human Genetic Studies. *PPAR Res* **2007**:83593.
- Itoh T, Fairall L, Amin K, Inaba Y, Szanto A, Balint Balint L, Nagy L, Yamamoto K and Schwabe John WR (2008) Structural basis for the activation of PPARgamma by oxidized fatty acids. *Nat Struct Mol Biol* **15**:924-931.
- Lu I-L, Huang C-F, Peng Y-H, Lin Y-T, Hsieh H-P, Chen C-T, Lien T-W, Lee H-J, Mahindroo N, Prakash E, Yueh A, Chen H-Y, Goparaju CMV, Chen X, Liao C-C, Chao Y-S, Hsu JT-A and Wu S-Y (2006) Structure-based drug design of a novel family of PPAR $\gamma$  partial agonists: Virtual screening, x-ray crystallography, and in vitro/in vivo biological activities. *J Med Chem* **49**:2703-2712.
- Luquet S, Gaudel C, Holst D, Lopez-Soriano J, Jehl-Pietri C, Fredenrich A and Grimaldi PA (2005) Roles of PPAR delta in lipid absorption and metabolism: a new target for the treatment of type 2 diabetes. *Biochim Biophys Acta* **1740**:313-317.
- Markt P, Petersen RK, Flindt EN, Kristiansen K, Kirchmair J, Spitzer G, Distinto S, Schuster D, Wolber G, Laggner C and Langer T (2008) Discovery of novel PPAR ligands by a virtual screening approach based on pharmacophore modeling, 3D shape, and electrostatic similarity screening. *J Med Chem* **51**:6303-6317.

MOL 62141

- Markt P, Schuster D, Kirchmair J, Laggner C and Langer T (2007) Pharmacophore modeling and parallel screening for PPAR ligands. *J Comput Aided Mol Des* **21**:575-590.
- Marque FA, Simonelli F, Oliveira ARM, Gohr GL and Leal PC (1998) Oxidative Coupling of 4-Substituted 2-Methoxy Phenols Using Methyltributylammonium Permanganate in Dichloromethane. *Tetrahedron Letters* **39**:943-946.
- Miyazawa M and Hisama M (2003) Antimutagenic Activity of Phenylpropanoids from Clove (*Syzygium aromaticum*). *Journal of Agricultural and Food Chemistry* **51**:6413-6422.
- Molecular\_Networks (2009) CORINA, Erlangen, Germany.
- Murakami Y, Shoji M, Hanazawa S, Tanaka S and Fujisawa S (2003) Preventive effect of bis-eugenol, a eugenol ortho dimer, on lipopolysaccharide-stimulated nuclear factor kappa B activation and inflammatory cytokine expression in macrophages. *Biochemical Pharmacology* **66**:1061-1066.
- Newman DJ and Cragg GM (2007) Natural products as sources of new drugs over the last 25 years. *J Nat Prod* **70**:461-477.
- Ogata M, Hoshi M, Urano S and Endo T (2000) Antioxidant activity of eugenol and related monomeric and dimeric compounds. *Chem Pharm Bull* **48**:1467-1469.
- Rachez C, Gamble M, Chang CP, Atkins GB, Lazar MA and Freedman LP (2000) The DRIP complex and SRC-1/p160 coactivators share similar nuclear receptor binding determinants but constitute functionally distinct complexes. *Mol Cell Biol* **20**:2718-2726.
- Rizos CV, Elisaf MS, Mikhailidis DP and Liberopoulos EN (2009) How safe is the use of thiazolidinediones in clinical practice? *Expert Opin Drug Saf* **8**:15-32.
- Rollinger JM, Steindl TM, Schuster D, Kirchmair J, Anrain K, Ellmerer EP, Langer T, Stuppner H, Wutzler P and Schmidtke M (2008) Structure-based virtual screening



MOL 62141

for the discovery of natural inhibitors for human rhinovirus coat protein. *J Med Chem* **51**:842-851.

Rosen ED, Sarraf P, Troy AE, Bradwin G, Moore K, Milstone DS, Spiegelman BM and Mortensen RM (1999) PPAR gamma is required for the differentiation of adipose tissue in vivo and in vitro. *Mol Cell* **4**:611-617.

Sohn EJ, Kim CS, Kim YS, Jung DH, Jang DS, Lee YM and Kim JS (2007) Effects of magnolol (5,5'-diallyl-2,2'-dihydroxybiphenyl) on diabetic nephropathy in type 2 diabetic Goto-Kakizaki rats. *Life Sci* **80**:468-475.

Tenenbaum A, Fisman EZ and Motro M (2003) Metabolic syndrome and type 2 diabetes mellitus: focus on peroxisome proliferator activated receptors (PPAR). *Cardiovasc Diabetol* **2**:4.

Wolber G, Dornhofer AA and Langer T (2006) Efficient overlay of small organic molecules using 3D pharmacophores. *Journal of Computer-Aided Molecular Design* **20**:773-788.

Wolber G and Langer T (2001) Comb(i)Gen: A novel software package for the rapid generation of virtual combinatorial libraries. *Rational Approaches to Drug Design*:390-399.

Wolber G and Langer T (2005) LigandScout: 3-D pharmacophores derived from protein-bound ligands and their use as virtual screening filters. *J Chem Inf Model* **45**:160-169.

Wright HM, Clish CB, Mikami T, Hauser S, Yanagi K, Hiramatsu R, Serhan CN and Spiegelman BM (2000) A synthetic antagonist for the peroxisome proliferator-activated receptor gamma inhibits adipocyte differentiation. *J Biol Chem* **275**:1873-1877.

MOL 62141

- Yahara S, Nishiyori T, Kohda A, Nohara T and Nishioka I (1991) Isolation and characterization of phenolic compounds from magnoliae cortex produced in China. *Chem Pharm Bull* **39**:2024-2036.
- Yu S and Reddy JK (2007) Transcription coactivators for peroxisome proliferator-activated receptors. *Biochim Biophys Acta* **1771**:936-951.
- Yumuk VD (2006) Targeting components of the stress system as potential therapies for the metabolic syndrome: the peroxisome-proliferator-activated receptors. *Ann N Y Acad Sci* **1083**:306-318.

MOL 62141

## Footnotes

### Sources of financial support:

This work was supported by grants from the Austrian Science Fund (FWF). [NFN S10704-B03, S10702-B03, and S10703-B03] and the Austrian Federal Ministry for Science and Research [ACM-2007-00178, ACM-2008-00857, and ACM-2009-01206]

### Numbered footnotes:

<sup>1</sup> N. F. and A. L. contributed equally to the present study.

<sup>2</sup> N. F. is a permanent member of the Faculty of Pharmacy, Gadjah Mada University, Sekip Utara, Yogyakarta 55281, Indonesia

MOL 62141

## Legends to figures

**Figure 1. Chemical structures of the compounds selected for pharmacological investigation.**

**Figure 2. PPAR $\gamma$  ligand binding potential of neolignans.** Serial dilutions of the tested compounds were prepared in DMSO and then mixed with a buffer solution containing the hPPAR $\gamma$  LBD tagged with GST, terbium-labelled anti-GST antibody, and fluorescently-labelled PPAR $\gamma$  agonist. After 1 h of incubation, the ability of the test compounds to bind to the PPAR $\gamma$  LBD and thus displace the fluorescently labelled ligand was estimated from the decrease of the emission ratio 520 nm/495 nm upon excitation at 340 nm. Each data point represents the mean  $\pm$  SD from three independent experiments performed in duplicate.

**Figure 3. Influence of the neolignans on the hPPAR $\gamma$ -mediated reporter gene transactivation.** HEK-293 cells, transiently cotransfected with a plasmid encoding full-length hPPAR $\gamma$ , a reporter plasmid containing PPRE coupled to a luciferase reporter and EGFP as internal control, were stimulated with the indicated concentrations of the respective compounds for 18 h. Luciferase activity was normalized by the EGFP-derived fluorescence, and the result was expressed as a fold induction compared to the negative control (DMSO vehicle treatment). The data shown are means  $\pm$  SD of three independent experiments each performed in quadruplet.

**Figure 4. Influence of neolignans on PPAR $\gamma$  coactivator recruitment.** The ability of the hPPAR $\gamma$ -ligand complex formed with the test compounds to recruit the TRAP220/DRIP-2

MOL 62141

coactivator peptide was measured as described in detail in the *Materials and Methods* section. Serial dilutions of the tested compounds were prepared in DMSO and then mixed with a buffer solution containing the hPPAR $\gamma$  LBD tagged with GST, terbium-labelled anti-GST antibody, and fluorescein-labelled TRAP220/DRIP-2 coactivator peptide. After incubation for 1 h, the emission at 520 nm and 495 nm after excitation at 340 nm was measured, and the 520 nm/495 nm ratio was used as a measure for the TRAP220/DRIP-2 coactivator recruitment potential of the respective compounds. Each data point represents the mean  $\pm$  SD from three independent experiments performed in duplicate.

**Figure 5. Putative interactions between the hPPAR $\gamma$  binding pocket and the neolignans 1 (A), 2 (B), and 3 (C).** The docking results were visualized using the LigandScout software with the following colour code: hydrogen bond acceptor (red arrow), hydrogen bond donor (green arrow), hydrophobic interaction (yellow sphere) and aromatic interaction (blue rings). The ligand binding pocket was depicted as surface coloured based on the hydrophilicity/lipophilicity.

**Figure 6. Adipogenic activity of compounds 1-4.** (A) 3T3-L1 preadipocytes were differentiated to adipocytes as described in the *Materials and Methods* section. After 7-8 days of differentiation with the indicated test compounds (1  $\mu$ M rosiglitazone, 50  $\mu$ M BADGE, and 10  $\mu$ M of the neolignans, respectively), Oil Red O staining was performed in order to clearly visualize the accumulated lipids. Representative photos of one experiment out of three with consistent results are depicted. (B) In order to get a quantitative measure, the dye accumulated in the cells (treated as described under A) was solubilized by 100% isopropanol and photometrically quantified at 550 nm. The data shown are means  $\pm$  SD from three independent experiments. \*  $p < 0.05$  and \*\*\*  $p < 0.001$ , as estimated by two-tailed paired t-test.

MOL 62141

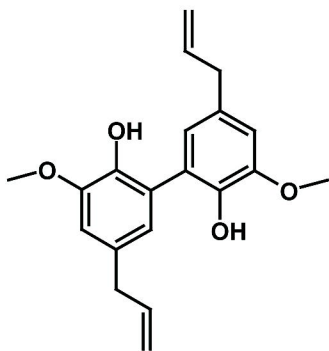
## Tables

**Table 1. Selectivity of the neolignans towards PPAR subtype (- $\alpha$ , - $\beta/\delta$ , - $\gamma$ )-driven luciferase reporter transactivation.**

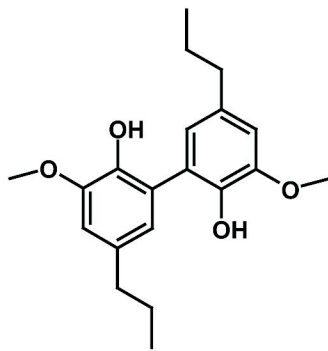
HEK-293 cells were transiently cotransfected with an expression plasmid for the respective PPAR subtype, a reporter plasmid containing PPRE coupled to the luciferase reporter, and EGFP as internal control. Cells were stimulated with the indicated concentrations of the respective compounds for 18 h. Luciferase activity was normalized by the EGFP-derived fluorescence, and the result was expressed as fold induction compared to the negative control (DMSO vehicle treatment). The selective agonists for PPAR $\alpha$  (GW7647), PPAR $\beta/\delta$  (GW0742), and PPAR $\gamma$  (pioglitazone), were used to verify the specificity of the respective assays. EC<sub>50</sub> and maximal fold activation were determined by the GraphPad Prism software version 4.03 (GraphPad Software Inc, USA) using settings for non linear regression with sigmoidal dose response and variable slope. The data shown represent means of three to five independent experiments each in quadruplet. ANOVA analysis showed statistical significance with  $p < 0.001$  for the presented effects.

	hPPAR $\alpha$		hPPAR $\beta/\delta$		hPPAR $\gamma$		mPPAR $\gamma$	
	EC <sub>50</sub> ( $\mu$ M)	maximal fold activation	EC <sub>50</sub> ( $\mu$ M)	maximal fold activation	EC <sub>50</sub> ( $\mu$ M)	maximal fold activation	EC <sub>50</sub> ( $\mu$ M)	maximal fold activation
<b>GW7647</b>	<b>0.0016</b>	<b>3.09</b>	-	-	-	-	-	-
<b>GW0742</b>	-	-	<b>0.0015</b>	<b>22.47</b>	-	-	-	-
<b>Pioglitazone</b>	-	-	-	-	<b>0.26</b>	<b>8.05</b>	<b>0.22</b>	<b>6.80</b>
<b>Dieugenol (1)</b>	n.d.	n.d.	n.d.	n.d.	<b>0.62</b>	<b>3.58</b>	<b>0.93</b>	<b>2.93</b>
<b>Tetrahydrodieugenol (2)</b>	n.d.	n.d.	n.d.	n.d.	<b>0.33</b>	<b>3.34</b>	<b>0.38</b>	<b>2.98</b>
<b>Magnolol (3)</b>	n.d.	n.d.	<b>11.41</b>	<b>2.45</b>	<b>1.62</b>	<b>3.03</b>	<b>1.14</b>	<b>2.81</b>
<b>Eugenol (4)</b>	n.d.	n.d.	n.d.	n.d.	n.d.	n.d.	n.d.	n.d.

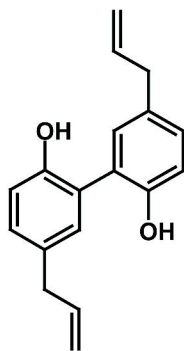
*n.d. not detected up to 100  $\mu$ M*



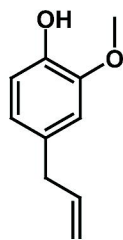
Dieugenol (1)



Tetrahydrodieugenol (2)



Magnolol (3)



Eugenol (4)

Figure 1

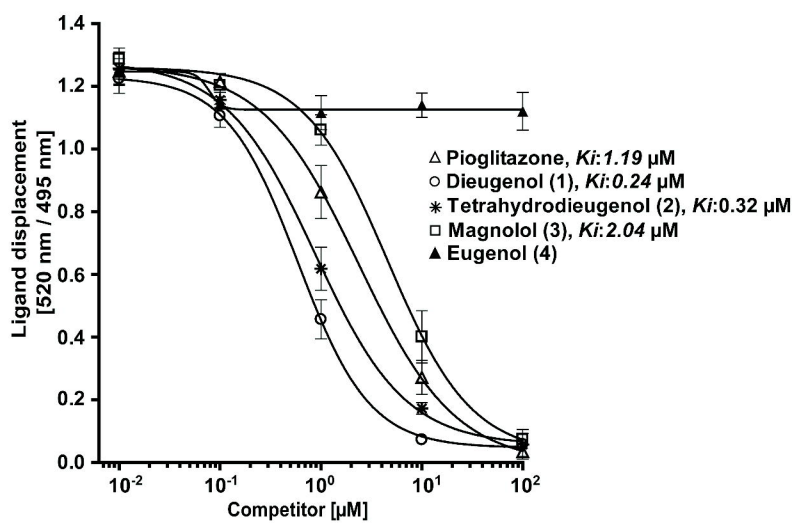


Figure 2



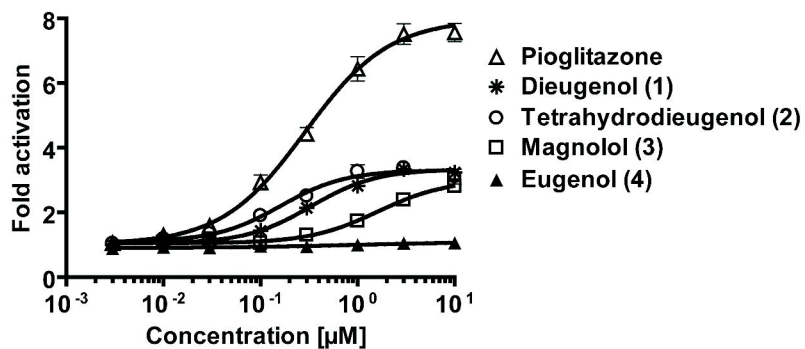


Figure 3

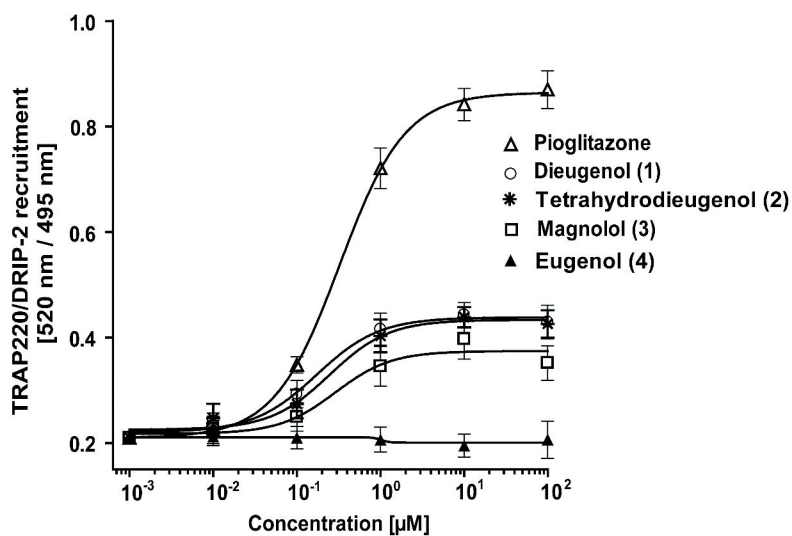
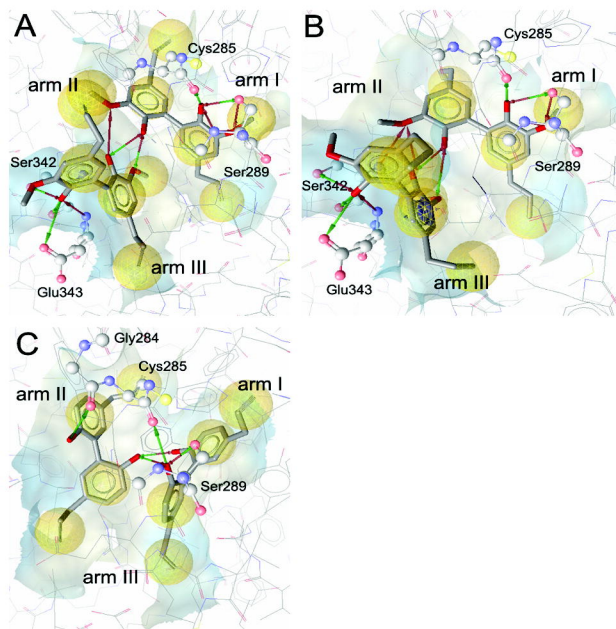
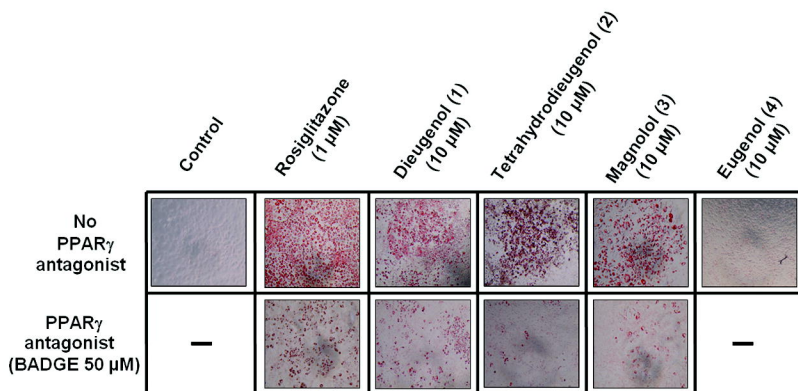


Figure 4



**Figure 5**

**A**



**B**

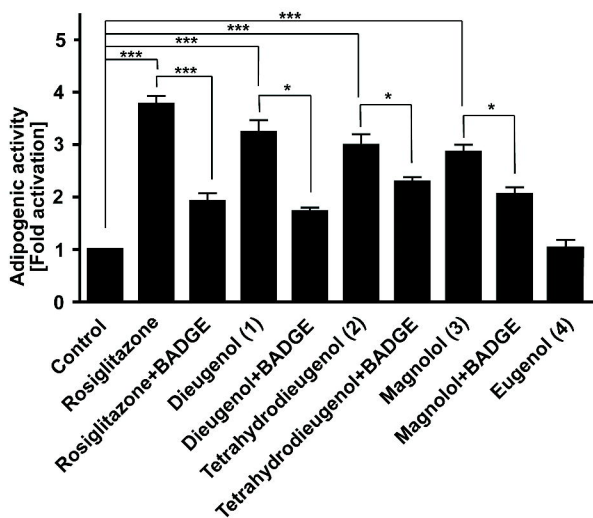


**Figure 6**